Optimal complexity and fractal limits of self-similar tensegrities

PROCEEDINGS A

Optimal complexity and fractal limits of self-similar tensegrities

Journal:	*Proceedings A*
Manuscript ID:	RSPA-2015-0250
Article Type:	Research
Date Submitted by the Author:	15-Apr-2015
Complete List of Authors:	De Tommasi, Domenico; Politecnico di Bari, DICAR Marano, Giuseppe; Politecnico di Bari, DICAR Puglisi, Giuseppe; Politecnico di Bari, Scienze dell'Ingegneria Civile e dell'Architettura Trentadue, Francesco; Politecnico di Bari, DICAR
Subject:	Structural engineering < ENGINEERING AND TECHNOLOGY
Keywords:	Tensegrities, Self-similar structures, Stability, Mass optimization

https://doi.org/10.1098/rspa.2015.0250
https://royalsocietypublishing.org/doi/10.1098/rspa.2015.0250
De Tommasi D., Marano G. C., Puglisi G. and Trentadue F. 2015Proc. R. Soc. A.471:20150250

PROCEEDINGS A

rspa.royalsocietypublishing.org

Research

Article submitted to journal

Subject Areas:
Structural engineering

Keywords:
Tensegrities, Self-similar structures, Stability, Mass optimization

Author for correspondence:
Francesco Trentadue
e-mail: francesco.trentadue@poliba.it

THE ROYAL SOCIETY PUBLISHING

Optimal complexity and fractal limits of self-similar tensegrities

D. De Tommasi[1], G.C. Marano[1], G. Puglisi[1], F. Trentadue[1]

[1] Dip. Scienze Ingegneria Civile e Architettura, Politecnico di Bari, Via Re David 200, Bari, Italy

We study the optimal (minimum mass) problem for a prototypical self-similar tensegrity column. By considering both global and local instability, we obtain that mass minimization corresponds to the contemporary attainment of instability at all scales. The optimal tensegrity depends on a dimensionless main physical parameter χ_0 that decreases as the tensegrity span increases or as the carried load decreases. As we show the optimal complexity (number of self-similar replication tensegrities) grows as χ_0 decreases with a fractal-like tensegrity limit. Then, we analytically determine a power law dependence of the optimal mass and complexity on the main parameter χ_0.

1. Introduction

The concept of *tensegrity*, first adopted by Fuller [13], is used to denote a specific class of light structures, consisting of compressed members (struts) connected by tensile cables, whose stability and shape depend on the prestretch of the tensile components. This structural class presents some specific, sometimes unique, characteristics that make it extremely attractive to realize lightweight, developable, and smart structures in different engineering fields. The first applications of the tensegrity concept were aimed at the design of light and elegant structures in Civil Engineering [3]. Afterwords, many new interesting applications in other fields have been proposed, based on the recalled attractive properties: deployable structures [9], [10], aerospace [6] and robotic [4] applications, sensors [5]. Finally the tensegrity concept has been observed in many biological systems such as cell cytoskeleton [2,11] and it is considered as an ubiquitous way for natural systems to transmit and control forces.

The crucial problem in the design and analysis of tensegrity structures is the study of instability effects: from one side the local buckling of struts, from the other side the (geometrical) global instability phenomena induced by the strong nonlinear dependence from the external loads and by the intrinsic non-unicity of the equilibrium problem (a typical effect in thin elastic structures, such as inflated spherical membranes, see *e.g.* [19]). Usual analyses of these systems have been based on the study of the only first type of instability (an exception can be find in [16] and [18] where both local and global stability are considered). Here we propose an optimization approach taking care of both local and global instability effects.

In particular, we consider the interesting case of hierarchical tensegrity structures obtained by a self-similar reproduction of a tensegrity basic element at different scales (see [14], [2]). To obtain analytical results, we focus on a plane tensegrity deduced starting by a T-bar [1] self-similar element (see Fig.1). The main novelty of our approach is to consider as *optimality condition* the contemporary attainment of a critical state at each scale. As we show, this full scale criticality is verified by the minimum mass tensegrity. A similar result has been obtained in [17] in the (nonlinear) mass optimization problem for truss structures, where the author shows that the optimal solution is characterised by a multimodal instability.

We obtain that the optimization problem is regulated by a main physical non dimensional parameter χ_0 that decreases as the tensegrity total length increases and/or as the carried load decreases. We then show the existence of an optimal complexity degree (number of self-similar subdivisions) and optimal shape, depending on χ_0 and on material parameters. Interestingly, we find that the complexity grows as χ_0 decreases. The dependence of optimal mass, prestress and geometry on the applied load and material properties are then explicitly analysed.

We then determine the dependence of the optimality solution from χ_0 and find power law relationships for both the optimal complexity and optimal mass. In particular we find that when $\chi_0 \to 0$ the tensegrity tends to a fractal-like limit structure, with an infinite refinement of the self-reproduction. Both the existence of a fractal limit and the signature of power laws inscribe our results in the framework of Self-Organized Criticality (SOC) with interesting analogies with other complex mechanical system (see *e.g.* [20], [21], [23] and references therein).

We point out that our results are of interest in the field of low loading and large length structures that in our model correspond to the described limit of $\chi_0 \to 0$. This situation occurs in particular in Space Engineering where low mass and deployability represent typically the most important design criteria [22]. Moreover we remark that our results are important also in the explanation of the observed complexity of many tensegrity biological systems observed at nano, micro and macro scales [2].

2. Mass optimization of a self-similar tensegrity column

As anticipated in the Introduction, the main novelty of the approach here proposed is an optimality criterion requiring the contemporary attainment of a critical state at all involved scales. This criterion will be confirmed by our analysis as a consequence of the Kuhn-Tucker conditions for the considered optimality problem. To get analytical results and show the importance of the analysis of both local and global stability, we focus on the simple explicit example of the plane tensegrity column represented in Fig.1.

In what follows we analyze the mass optimization within this class of tensegrities of increasing complexity, of fixed total length l_0 and under a fixed compressive load N_0.

(a) Single compressed bar

Consider first a single bar with cross section of area A_0 and of axial area moment $J_0 = \frac{A_0^2}{\xi^2 \pi^2}$ (here ξ depends only on the form of the cross section, *e.g.* $\xi^2 = \frac{4}{\pi}$ in the case of circular section). We fix

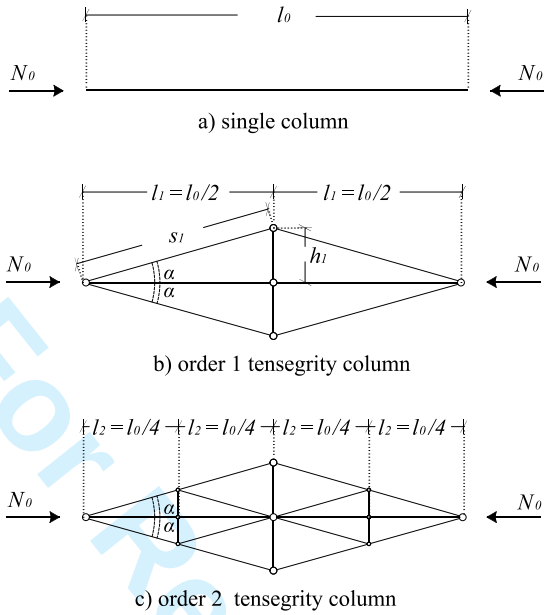

Figure 1. Scheme of the self-similar tensegrity column.

{figa}

A_0 by imposing that N_0 corresponds to the Eulerian critical load of the column:

$$A_0 = \xi\, l_0 \sqrt{\frac{N_0}{E}}. \tag{2.1}$$ {A0}

Further, we indicate as $\chi_0 = \frac{N_0}{\sigma_s A_0}$ the ratio between the Eulerian critical load an the compressive failure load (here σ_s is the compression failure stress). This dimensionless parameter will be the main parameter determining the optimal complexity. In view of (2.1), it can be written as

$$\chi_0 = \frac{\sqrt{E N_0}}{\sigma_s \xi\, l_0}. \tag{2.2}$$ {ko0}

If we assume that the compression failure load $\sigma_s A_0$ is greater than the Eulerian critical load ($\chi_0 < 1$), then the optimal mass of the column is

$$m_0 = m_b(l_0, N_0) = \rho\, \xi\, l_0^2 \sqrt{\frac{N_0}{E}},$$

where ρ is the mass density. Here we indicate by $m_b(l, N)$ the optimal mass preventing Eulerian buckling for a column of length l under a normal force N. Similarly we indicate by $m_s(l, N) = \rho\, \sigma_s\, A\, l$ the optimal mass preventing material failure.

Then the assumption $\chi_0 < 1$ impies

$$\chi_0 = \frac{N_0}{\sigma_s A_0} = \frac{m_s(l_0, N_0)}{m_b(l_0, N_0)} \leq 1. \tag{2.3}$$ {ko}

Observe also that χ_0 can be written as $\chi_0 = (\lambda_s/\lambda)^2$, where $\lambda = \frac{l_0}{\sqrt{J_0/A_0}}$ is the slenderness of the beam, whereas $\lambda_s = \sqrt{\frac{\pi^2 E}{\sigma_s}}$ is the value of the slenderness such that the critical Eulerian load and the material failure load coincide. Thus χ_0 measures the slenderness of the column and can be

decreased or by decreasing the assigned load N_0 (at fixed length) or by increasing the slenderness (at fixed load).

The second dimensionless parameter determining the optimal complexity is

$$\epsilon = \frac{\sigma_s}{E} \ll 1 \tag{2.4}$$ {eps}

This material parameter is here assumed as a smallness parameter. In particular in the following the assumption (2.4) allows us to identify the length of the bars in the deformed and undeformed configurations.

(b) Order one tensegrity column

Consider now a tensegrity column consisting, in the terminology of [1], in a T-bar (see Fig.1$_b$) characterized by the same length l_0 and the same compression load N_0 of the single column considered above. This structure is constituted by:

· four prestressed cables of length $s_1 = \frac{l_0}{2\cos\alpha}$, where α is the angle between the cables and the horizontal struts;

· two horizontal struts of length $l_1 = \frac{l_0}{2}$;

· two vertical struts of length $h_1 = \frac{l_0 \tan\alpha}{2}$.

All struts are assumed hinged and have the same shape of the cross-section (fixed ξ) of the zero order column. The tensegrity is prestressed and we describe the effect of prestrecthing on the loaded state by the dimensionless parameter:

$$\beta_1 = \frac{N_1}{N_0} > 1,$$

where N_1 is the compressive force in the two horizontal struts. By equilibrium considerations we find that the traction force on the four cables is $T_1 = \frac{\beta_1 - 1}{2\cos\alpha} N_0$, whereas the compressive force in the two vertical struts is $N_1^v = (\beta_1 - 1) N_0 \tan\alpha$. Both α and β_1 represent minimization (design) parameters.

Now, we apply our optimality criterion to determine the masses of the components of the T-bar. The optimal mass of a generic strut with length $l = a l_0$, carrying an axial force $N = b N_0$, is obtained by considering both the case in which N corresponds to its Eulerian critical load and the case in which N corresponds to its compression failure load. Thus in the first case we determine the optimal dimensionless mass

$$\mu_b = \mu_b(a,b) = \frac{m_b(a l_0, b N_0)}{m_b(l_0, N_0)} = a^2\sqrt{b}, \tag{2.5}$$ {mub}

while in the second case, using (2.3), the optimal dimensionless mass is given by

$$\mu_s = \mu_s(a,b) = \frac{m_s(a l_0, b N_0)}{m_b(l_0, N_0)} = \frac{m_s(l_0, N_0)}{m_b(l_0, N_0)} \frac{m_s(a l_0, b N_0)}{m_s(l_0, N_0)} = \chi_0\, ab. \tag{2.6}$$ {mus}

Thus the optimal dimensionless mass of the struts is

$$\mu = \mu(a,b) = \max\{\mu_b(a,b); \mu_s(a,b)\} = \max\{a^2\sqrt{b}; \chi_0\, ab\}.$$

Similarly the optimal dimensionless mass of a cable with length $l = a l_0$, carrying a traction force $N = b N_0$, is $\mu_s(a,b)$.

Here for simplicity of notation we assume that the cables are constituted by the same material of the struts, but the results can be easily extended to the more general case of different materials.

As a result, the dimensionless mass (with respect to $m_b(l_0, N_0)$) of the order one tensegrity is

$$\begin{aligned}\mu_1 &= 4\mu_s\left(\frac{1}{2\cos\alpha}, \frac{\beta_1-1}{2\cos\alpha}\right) + 2\mu\left(\frac{1}{2}, \beta_1\right)\\ &+ 2\mu\left(\frac{\tan\alpha}{2}, (\beta_1-1)\tan\alpha\right)\\ &= \chi_0(\beta_1-1)(\tan^2\alpha+1) + \max\left\{\chi_0\beta_1; \frac{\sqrt{\beta_1}}{2}\right\}\\ &+ \max\left\{\chi_0(\beta_1-1)\tan^2\alpha; \frac{\sqrt{\beta_1-1}}{2}(\tan\alpha)^{\frac{5}{2}}\right\}.\end{aligned} \tag{2.7}$$

{mu1}

(c) Higher order tensegrity column ($n > 1$)

The tensegrity column of order $n = 2$ is obtained (see Fig.1$_c$) by substituting in the previous order one tensegrity the two horizontal struts by two geometrically similar order one tensegrities (with length $l_1 = l_0/2$). In particular, we assume that each of the two, so introduced, order one tensegrities is subjected to the same force $\beta_1 N_0$ acting on the two removed horizontal struts and that $\beta_2^T N_0 = \beta_1\beta_2 N_0$ is the force acting on the new four horizontal struts of length $l_2 = l_0/4$. Thus β_2^T is the ratio between the forces acting on the four horizontal struts and the external load N_0.

By reiterating this procedure we obtain the tensegrity column of order n, constituted by the following elements:

· 2^n horizontal struts of length $l_n = \frac{l_0}{2^n}$ undergoing the (compression) force $N_n = \beta_n^T N_0 = \Pi_{i=1}^n \beta_i N_0$;

· $\sum_{i=1}^n 2^{i+1}$ cables of variable lengths $s_i = \frac{l_0}{2^i\cos\alpha}$, undergoing the traction forces $T_i = \frac{(\beta-1)\beta_{i-1}^T}{2\cos\alpha} N_0$;

· $\sum_{i=1}^n 2^i$ vertical struts also of variable lengths $l_i^v = \frac{l_0\tan\alpha}{2^i}$, undergoing the forces $N_i^v = (\beta_i - 1)\beta_{i-1}^T N_0\tan\alpha$.

Thus the (dimensionless) mass μ_n at the complexity n is

$$\begin{aligned}\mu_n &= 2^n\mu\left(\frac{1}{2^n}, \beta_n^T\right) + \sum_{i=1}^n 2^{i+1}\mu_s\left(\frac{1}{2^i\cos\alpha}, \frac{(\beta_i-1)\beta_{i-1}^T}{2\cos\alpha}\right)\\ &+ \sum_{i=1}^n 2^i\mu\left(\frac{\tan\alpha}{2^i}, (\beta_i-1)\beta_{i-1}^T\tan\alpha\right)\\ &= \max\left\{\frac{\sqrt{\beta_n^T}}{2^n}, \chi_0\beta_n^T\right\} + \sum_{i=1}^n\left[\chi_0(\beta_i-1)\beta_{i-1}^T(1+\tan^2\alpha)\right.\\ &+ \left.\max\left\{\frac{\tan^{\frac{5}{2}}\alpha}{2^i}\sqrt{(\beta_i-1)\beta_{i-1}^T}, \chi_0(\beta_i-1)\beta_{i-1}^T\tan^2\alpha\right\}\right].\end{aligned} \tag{2.8}$$

{resb}

3. Global stability

In this section we study the global stability problem for the tensegrity of complexity n. Again we begin by analyzing an order one tensegrity to deduce, by an iterative method, stability results for the order n complexity. Subsequently, we are able to optimize the parameters β_i defining the prestretching and the geometrical parameter α.

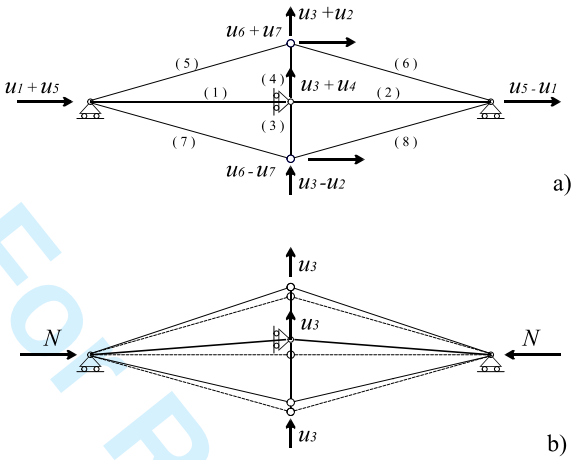

Figure 2. Scheme of the global stability. a) Lagrangean variables, b) critical mode.

{figb}

(a) Order one tensegrity

Consider an order one tensegrity of length l, subjected to an axial force N. We choose as Lagrangian parameters the *generalized* node displacements u_i (see Fig.2a), measuring the incremental displacements from the prestressed, loaded configuration. By considering the symmetry properties of the system, these variables are chosen symmetric or antisymmetric with respect to both the vertical axes and the horizontal axes.

The total potential energy (set equal to zero in the prestressed loaded state) of the generic order one tensegrity structure can be written as

$$V(\boldsymbol{u},N)=\sum_{k=1}^{8}\left[N^{(k)}\Delta l^{(k)}+\frac{EA^{(k)}}{2}\left(\frac{\Delta l^{(k)}}{l^{(k)}}\right)^2 l^{(k)}\right]-2Nu_1, \tag{3.1}$$

{eq1}

where

$$\Delta l^{(k)}=||\Delta \boldsymbol{x}^{(k)}+\boldsymbol{T}^{(k)}\boldsymbol{u}||-l^{(k)}.$$

Here $l^{(k)}$ are the lengths of the members with area $A^{(k)}$ and $\Delta l^{(k)}$ are their elongations, whereas $\Delta \boldsymbol{x}^{(k)}$ and $\boldsymbol{T}^{(k)}\boldsymbol{u}$ are the axial vector in the reference configuration and the relative incremental displacement vector between the end joints of the (k)-th bar, respectively. As already stated, in view of the assumption (2.4) we identify the deformed lengths of the bars with the natural ones.

We assume, according with the so called *maximum delay convention* [15], that the system stays in a (metastable) equilibrium configuration until it disappears. This is classical in structures bifurcation stability analyses, but other possible hypotheses, *e.g.* assuming that the configurations of the system correspond to the global energy minimum, can be considered (*e.g.* Maxwell convention [22]). Under this assumption we study the positiveness of the Hessian (tangent stiffness) matrix

$$\boldsymbol{K}=\frac{\partial^2 V}{\partial \boldsymbol{u}\partial \boldsymbol{u}}\bigg|_{\boldsymbol{u}=\boldsymbol{0}}\succ 0 \tag{3.2}$$

{eq2}

that, based on our choice of the Lagrangian variables is a block diagonal matrix

$$\boldsymbol{K} = \begin{bmatrix} \boldsymbol{K}_{ss} & & & \\ & \boldsymbol{K}_{as} & \boldsymbol{0} & \\ & \boldsymbol{0} & \boldsymbol{K}_{sa} & \\ & & & K_{aa} \end{bmatrix}. \tag{3.3}$$ {eq3}

Here $\boldsymbol{K}_{ss}$, $\boldsymbol{K}_{as}$, and $\boldsymbol{K}_{sa}$ are 2×2 square matrices whereas K_{aa} is a scalar. The double index notation indicates the symmetric (s) and antisymmetric (a) properties (see Fig.2), with the first index referring to the horizontal axes and the second index to the vertical axes. In particular, u_1 and u_2 are *ss* variables, u_3 and u_4 are *as* variables, u_5 and u_6 are *sa* variables and u_7 is an *aa* variable. We refer to the Appendix 1 for all details and for the explicit deduction of $\boldsymbol{K}$.

The proposed approach let us obtain numerically the solution of the optimal mass problem for the generic tensegrity. However, in the following, to obtain analytical results, we assume (see again the Appendix 1 for a justification of this hypothesis) that

$$\phi = \frac{N}{El^2} \ll 1. \tag{3.4}$$ {hypp}

Indeed, under this hypothesis we obtain that only one of the eigenvalues of $\boldsymbol{K}_{as}$ can be negative whereas all other eigenvalues of $\boldsymbol{K}$ are positive (see again the Appendix 1). This eigenvalue takes the form

$$\lambda_{as1} = \frac{4El\left((\beta_1 - 1)\tan^2\alpha - \epsilon\left(\beta_1 \tan^2\alpha + 1\right)\right)}{\epsilon\left(\tan^2\alpha + 1\right)}\phi \tag{3.5}$$ {eig}

and it is associated to the critical mode represented in Fig.2_b.

Thus, using (3.5), we deduce that under the hypothesis (3.4) the order one tensegrity is stable iff

$$\tan\alpha > \eta(\beta_1) := \sqrt{\frac{\epsilon}{(\beta_1 - 1) - \beta\epsilon}}. \tag{3.6}$$ {etabeta}

(b) Higher order tensegrities

To extend the above results to higher complexity tensegrities, we first observe that the stability result (3.6) does not depend from the length of the tensegrity, from the applied load and (see Appendix 1 for details) from the stiffnesses of the struts.

Consider first the order two tensegrity. To study the stability of the single two T-bars with length $l_0/2$ (see Fig.1_c) subjected to the forces $N_1 = \beta_1 N_0$, we begin by observing that the stability result (3.6) can be applied also in this case. As a result the stability of the two T-bars is ensured by the relation

$$\eta(\beta_2) < \tan\alpha. \tag{3.7}$$ {h1}

Then, the global stability of the order two tensegrity, can be analysed by substituting the two T-bars by *equivalent* struts with identical elastic stiffness. Thus we reduce the stability analysis of the order two tensegrity to the stability analysis of this equivalent order one tensegrity. We obtain then the second stability condition

$$\eta(\beta_1) < \tan\alpha. \tag{3.8}$$ {h2}

Therefore the stability of the order two tensegrity is granted by the simultaneous fulfillment of (3.7) and (3.8).

The stability of the tensegrity of order n is then be simply obtained by reiterating this approach. We obtain thus that the tensegrity is stable iff

$$\eta(\beta_i) < \tan\alpha, \qquad i = 1, ..., n. \tag{3.9}$$ {hn}

4. Optimal geometry, complexity, and prestretching

In order to perform the mass optimization analysis, we begin by observing that the optimal design for the order n tensegrity is obtained by ensuring the contemporary attainment of instability at all the scales. This corresponds to the following conditions:

$$\eta(\beta_i) = \tan\alpha, \;\; i = 1, ..., n. \tag{4.1}$$ {opt}

Indeed the optimality problem

$$\min_{\tan\alpha - \eta(\beta_i) \geq 0} \;\; \mu_n(\tan\alpha, \beta_i) \tag{4.2}$$ {min}

leads to the classical Kuhn-Tucker conditions [7]

$$\begin{aligned} &\frac{\partial \mu_n}{\partial \tan\alpha} = \sum_{i=1}^{n} \lambda_i, \\ &\frac{\partial \mu_n}{\partial \beta_i} = -\lambda_i \frac{d\eta(\beta_i)}{d\beta_i}, \qquad i = 1, ..., n, \\ &\lambda_i(\tan\alpha - \eta(\beta_i)) = 0, \qquad i = 1, ..., n, \\ &\lambda_i \geq 0, \qquad i = 1, ..., n. \end{aligned} \tag{4.3}$$ {KT}

Since $\frac{\partial \mu_n}{\partial \tan\alpha} > 0$, $\frac{\partial \mu_n}{\partial \beta_i} > 0$ for $i = 1, ..., n$, and $\frac{d\eta}{d\beta} < 0$ (4.3) are satisfied if $\eta(\beta_i) = \tan\alpha$, $i = 1, ..., n$, we obtain the optimality conditions (4.1).

Notice that the optimal prestretch parameters β_i are scale invariant and using (3.6) are given by

$$\beta_1 = ... = \beta_n = \eta^{-1}(\tan(\alpha)) := \frac{\epsilon + \tan^2\alpha}{\tan^2\alpha\,(1-\epsilon)}. \tag{4.4}$$ {bet}

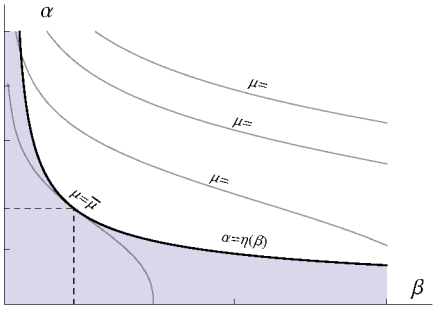

Figure 3. Geometrical construction of the optimal configuration for $n = 1$. With the shadowed area we represent the unstable states, whereas continuous thin lines are the contour lines of the mass ratio μ for the case $n = 1$. Here $\epsilon = 10^{-3}$ and $\chi_0 = 0.1$.

{Fig3}

In Fig.3 we show the solution of (4.2), for the simple case of $n = 1$. Here we plot the boundary $\tan\alpha = \eta(\beta)$ of the stability domain (grey area represents unstable states) and the contour lines of the dimensionless mass μ_1. *The optimal point* $(\bar{\alpha}_n, \bar{\beta}_n)$ and the corresponding *optimal mass* $\bar{\mu}_n$ is geometrically obtained by a tangency condition between the optimal curve (3.6) and the contour lines of μ_1. Of course, this geometric condition descends again by the Kuhn-Tucker conditions (4.3) and corresponds to the minimization with respect to $\tan\alpha$ of the expression (2.8) after substituting the conditions (4.4).

The optimal mass and complexity is then obtained by minimizing with respect to the complexity parameter n. We indicate by α_{opt}, β_{opt} and μ_{opt} the solutions of the optimal complexity determined by

$$\mu_{opt} = \min_n \mu_n\big(\bar{\beta}_n, \tan\bar{\alpha}_n\big).$$

This minimization is described in Fig.4, for the two values $\epsilon = 10^{-3}$ and $\epsilon = 10^{-2}$ of the material parameter in (2.4). The different curves correspond to different values of the dimensionless load χ_0 in (2.3). Observe that for high values of χ_0, *i.e.* when the Eulerian load N_0 approaches the material failure load, the optimum mass corresponds to a low complexity or even to the single compressed column. On the contrary the complexity grows as χ_0 decreases, *i.e.* when N_0 decreases or the slenderness of the column grows.

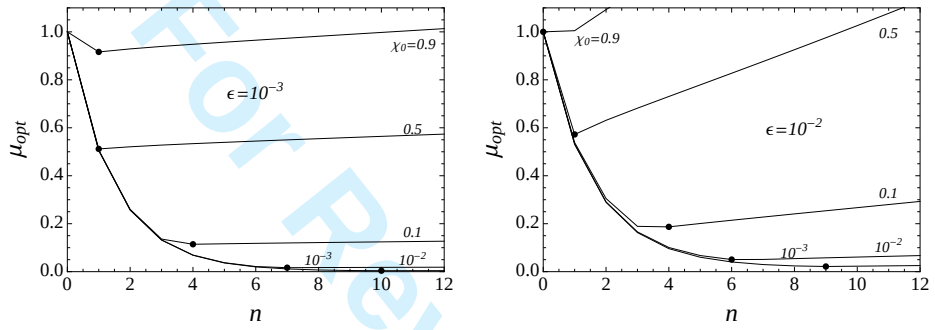

Figure 4. Optimal value of the mass as a function of the complexity n. Each curve is labelled by the values of the non dimensional load χ_0 in (2.3) for two different values of the smallness material parameter ϵ in (2.4).

{fig4}

These results are synthesized in Fig.5a where the optimal complexity n_{opt} and the corresponding optimal mass μ_{opt} are represented as functions of the slenderness parameter χ_0. Again the figure shows that the optimal complexity increases as χ_0 decreases. The figure also shows that the optimal complexity grows as the non dimensional material parameter ϵ decreases.

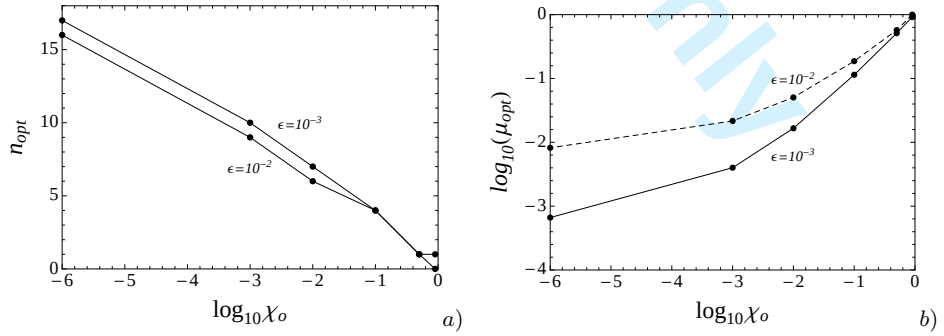

Figure 5. Dependence of the optimal complexity and optimal mass from the non dimensional stress χ_0 in (2.3) for two different values of the smallness material parameter ϵ in (2.4).

{fig5}

It is interesting to observe (see Appendix 2) that the optimal complexity n_{opt} is attained at the lowest complexity leading to the transition from Eulerian buckling to material failure in the horizontal struts.

Finally, the analysis of Fig.5$_b$ shows that the non-dimensional mass μ_{opt} decreases as the slenderness increases and as the material parameter ϵ decreases. This can also be deduced by observing that in Fig.3 only the boundary of the stability domain changes, according with (4.4), moving upwards as ϵ increases. Also in Fig.6 we represent the dependence of the optimal prestress β_{opt} and of the angle α_{opt} from both χ_0 and ε.

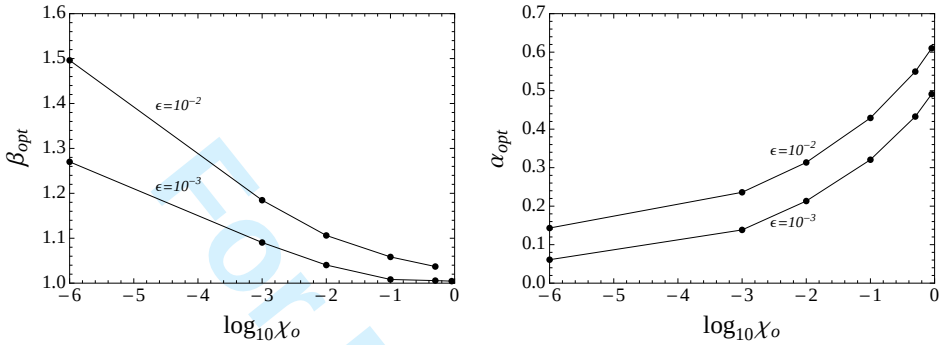

Figure 6. Optimal values of the prestress parameter β and of the angle α as functions of χ_0 for two different values of ϵ.

{fig6}

5. Fractal limits and self organized criticality

In this section we study the important limit case of $\chi_0 \to 0$ (limit of infinite tensegrity span or of infinitesimal carried load) that, as the numerical analysis in the previous section shows, determines an increasing optimal complexity. To obtain analytical results, we here fix the geometrical parameter α (and consequently β according with the optimization condition (4.4)).

Under this hypothesis it is possible to define analytically the optimal complexity. More precisely, it is possible to show (see the Propositions 1 and 2 in Appendix 2) that if the material parameter ε is small enough (say $\varepsilon = 10^{-2}$), we can find an open interval $I_\varepsilon = (\alpha_1(\varepsilon),\ \alpha_2(\varepsilon))$ of the angle α (say $I_{10^{-2}} = (0.047\pi, 0.461\pi)$) such that if $\alpha \in I_\varepsilon$ then

$$\text{int}\,(\nu) \le n_{opt} \le \text{int}\,(\nu) + 1, \tag{5.1}$$ {incastro}

where

$$\nu = -\frac{\log_{10}\chi_0}{\log_{10} 2\sqrt{\beta}}. \tag{5.2}$$ {nu0}

Remark. The inequalities (5.1) show that at the optimal complexity n_{opt} a transition occurs from Eulerian buckling to material failure in the horizontal struts. In other words, the optimal mass is attained or in the highest complexity leading to Eulerian buckling or in the lowest complexity leading to material failure. Thus, in particular, the replacement of a simple horizontal strut with a T-bar of the same length is convenient only if the crisis of the strut is due to buckling.

In Fig.7$_a$ we show the linear dependence of the optimal complexity parameter ν on $\log_{10}(\chi_0)$. Interestingly, we obtain a linear dependence of the complexity on $\log_{10}(\chi_0)$ with a power law dependence between the optimal mass

$$\mu_{n_{opt}} = \min\{\,\mu_{\text{int}(\nu)}, \mu_{\text{int}(\nu)+1}\,\}$$

and the parameter χ_0 shown in Fig.7$_b$ with a linear log-log dependence for about three different scales.

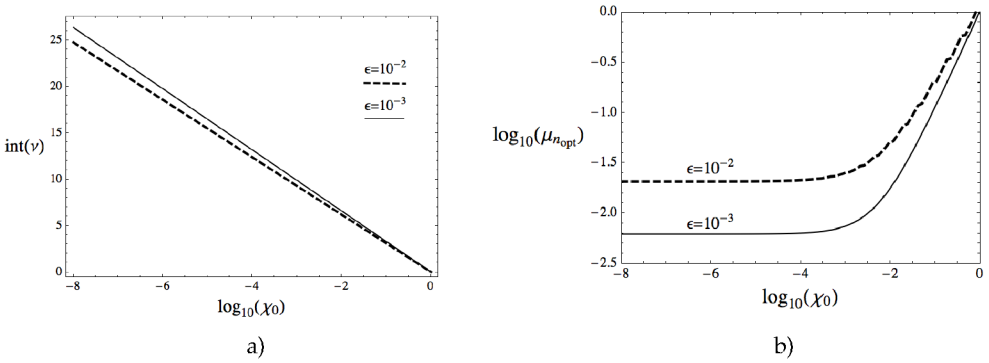

Figure 7. Dependence of the optimal complexity a) and of the optimal mass b) on the parameter χ_0. Here we assumed $\alpha = 0.1\pi$.

{fig10}

Observe that for small values of χ_0 the power law is not respected. We argue that this feature is due to our simplifying approach based on the self similarity of the only horizontal struts and not of the vertical ones. In order to support this statement, in Fig.8 we reported by the thin line the mass μ_{hs-c} of only horizontal struts and cables, without considering the mass of the vertical struts. As the figure shows, the range where power law is respected, coincide with the range where the mass of vertical struts can be neglected.

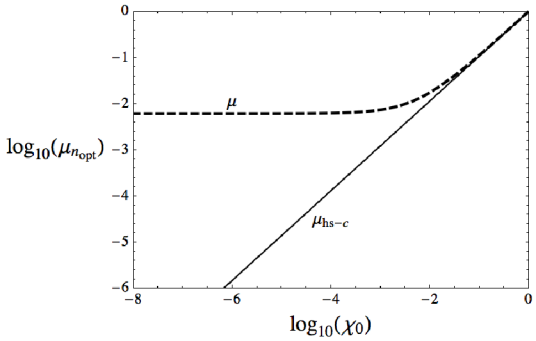

Figure 8. Comparison of the total mass μ and the mass μ_{hs-c} of the horizontal struts and cables (without the mass vertical struts). Here $\varepsilon = 10^{-3}$ and $\alpha = 0.1\pi$.

{fig11}

These results naturally refer our optimization problem, leading to a contemporary criticality at all scales, to the theory of Self Organized Criticality [20]. In particular we remark that, in view of (2.2), for fixed length, section shape and material parameters, χ_0 decreases as the applied compressive load N_0 decreases. Interestingly, in the limit case of a vanishing normal compressive force we find that the optimal tensegrity exhibits a fractal nature. A similar result is obtained if for fixed N_0 we increase the length of the column.

Finally, in Fig.9 we study the dependence of the critical exponent regulating the power law (5.2) from the angle α and from the constitutive parameter ε.

Funding statement. The work G.P. and D.D. has been supported by Fondi di Ricerca di Ateneo of Politecnico di Bari.

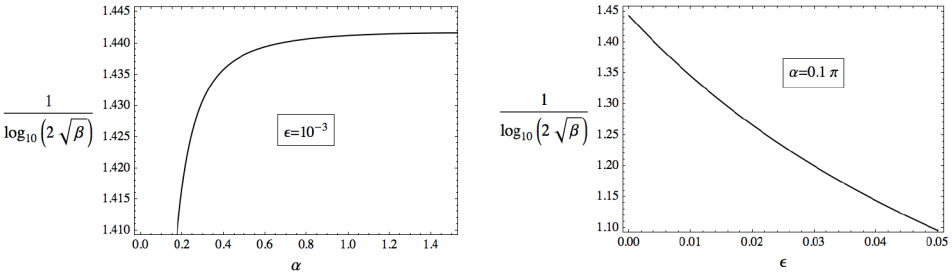

Figure 9. Dependence of the critical exponent a) from the angle α and b) from the constitutive parameter ε.

{fig12}

Appendix 1

In this Appendix we give the details of the global stability analysis (see Section 3) for the tensegrity shown in Fig.2. The submatrices in the tangent stiffness matrix (3.3) have the following expressions:

$$\boldsymbol{K}_{ss} = 2\begin{bmatrix} (k_{es}-k_{gs})\cos 2\alpha + k_{eh} + k_{es} + k_{gs} & (k_{gs}-k_{es})\sin 2\alpha \\ (k_{gs}-k_{es})\sin 2\alpha & (k_{gs}-k_{es})\cos 2\alpha + k_{eh} + k_{es} + k_{gs} \end{bmatrix}$$

$$\boldsymbol{K}_{sa} = 2\begin{bmatrix} (k_{gs}-k_{es})\cos 2\alpha + k_{gh} + k_{es} + k_{gs} & k_{gh} \\ k_{gh} & k_{ev} + k_{gh} \end{bmatrix}$$

$$\boldsymbol{K}_{as} = 2\begin{bmatrix} (k_{es}-k_{gs})\cos 2\alpha + k_{eh} + k_{es} + k_{gs} & (k_{es}-k_{gs})\cos 2\alpha + k_{gs} + k_{es} \\ (k_{es}-k_{gs})\cos 2\alpha + k_{gs} + k_{es} & (k_{es}-k_{gs})\cos 2\alpha + k_{gv} + k_{es} + k_{gs} \end{bmatrix}$$

$$K_{aa} = 2((k_{es}-k_{gs})\cos 2\alpha + k_{gv} + k_{es} + k_{gs}).$$

Here we have indicated by k_{eh} and k_{gh} the elastic stiffness and the geometric stiffness of the horizontal struts:

$$\begin{aligned} k_{eh} &= \frac{EA^{(k)}}{l^{(k)}} = \nu_h\,\xi\sqrt{\beta\,E\,N}, \qquad k = 1, 2, \\ k_{gh} &= \frac{N^{(k)}}{l^{(k)}} = -\frac{2\beta N}{l}. \end{aligned} \tag{5.3}$$

Notice that, since the two horizontal struts can represent also *equivalent* struts or can be designed against material failure, $A^{(1)}$ and $A^{(2)}$ are expressed as

$$A^{(1)} = A^{(2)} = \nu_h \xi \frac{l}{2}\sqrt{\frac{\beta N}{E}}$$

where $\nu_h > 0$ is the ratio between the actual cross section and the cross section area preventing the buckling failure.

Further, we have indicated by k_{ev} and k_{gv} the elastic stiffness and the geometric stiffness of the vertical struts:

$$\begin{aligned} k_{ev} &= \frac{EA^{(k)}}{l^{(k)}} = \nu_v\xi\sqrt{(\beta-1)E\,N\tan\alpha}, \qquad k = 3, 4, \\ k_{gv} &= \frac{N^{(k)}}{l^{(k)}} = -\frac{2(\beta-1)N}{l}. \end{aligned} \tag{5.4}$$

Here, since the two vertical struts can be also designed against material failure,

$$A^{(3)} = A^{(4)} = \nu_v \, \xi \frac{l}{2 \tan \alpha} \sqrt{\frac{(\beta - 1) N \tan \alpha}{E}}$$

where $\nu_v > 0$ has the same meaning of ν_h introduced above.

Finally, we have indicated by k_{es} and k_{gs} the elastic stiffness and the geometric stiffness of the strings:

$$\begin{aligned} k_{es} &= \frac{E A^{(k)}}{l^{(k)}} = \frac{E(\beta - 1)\, N}{\sigma l}, \qquad k = 5, 6, 7, 8, \\ k_{gs} &= \frac{N^{(k)}}{l^{(k)}} = \frac{(\beta - 1) N}{l}. \end{aligned} \tag{5.5}$$

Here the cross sections areas are designed again material failure

$$A^{(k)} = \frac{(\beta - 1)\, N}{2 \sigma \cos \alpha} \qquad k = 5, 6, 7, 8.$$

Of course a numerical analysis let us analyze the positivity conditions $\boldsymbol{K} \succ \boldsymbol{0}$. However, to determine analytically the critical mode and to study the positiveness of $\boldsymbol{K}$ we introduce the smallness parameter

$$\phi = \frac{N}{E l^2} \ll 1. \tag{5.6}$$ {ip}

Indeed, we may observe that

$$\phi = \frac{N}{E l^2} \leq \frac{\sigma_s A^{(1)}}{\beta E l^2} = \frac{\epsilon}{\beta} \frac{A^{(1)}}{l^2},$$

where ϵ is the small parameter introduced in (2.4). Of course also the second fraction is small for a slender bar.

After easy computations we obtain (up to higher order terms) the eigenvalues

$$\begin{aligned} \lambda_{ss1} &= \lambda_{sa1} = \frac{2\sqrt{\beta} E l \nu_h \xi}{\pi} \sqrt{\phi}; \\ \lambda_{ss2} &= \lambda_{as2} = \frac{2 E l \nu_v \xi \sqrt{(\beta - 1) \tan \alpha}}{\pi} \sqrt{\phi}; \\ \lambda_{as1} &= \frac{4 E l \left((\beta - 1) \tan^2 \alpha - \epsilon \left(\beta \tan^2 \alpha + 1 \right) \right)}{\epsilon \left(\tan^2 \alpha + 1 \right)} \phi; \\ \lambda_{sa2} &= \lambda_{aa} = \frac{4 E l (\beta - 1)(E - \sigma)}{\sigma \left(\tan^2 \alpha + 1 \right)} \phi \end{aligned}$$

We can note that all the eigenvalues are positive, with the exception of λ_{as1} that is positive iff

$$\tan \alpha > \eta(\beta) = \sqrt{\frac{\epsilon}{(\beta - 1) - \epsilon \beta}}.$$

Finally, it is worth noting that, under the smallness assumptions (5.6), the stability results here established are independent by the applied load. In this regard we recall that the bar cross sections are not fixed, but are designed on the base of the applied load.

Appendix 2

In this Appendix we obtain the results we adopt to analyze the case $\chi_0 \to 0$ in Section 5.

Proposition 1 *The optimal complexity n_{opt} verifies $n_{opt} \leq 1 + \mathrm{int}(\nu)$, where*

$$\nu = -\frac{\log_{10} \chi_0}{\log_{10} 2\sqrt{\beta}}. \tag{5.7}$$ {nu}

Proof. We begin by defining the dimensionless mass increment

$$\Delta\mu_n = \mu_n - \mu_{n-1} \tag{5.8}$$ {del0}

between the complexity $n-1$ and n. Further, we denote by χ_j the ratio between the minimal mass preventing material failure and the minimal mass preventing buckling in the horizontal struts at the complexity order j:

$$\chi_j = \frac{m_s(l_j, \beta^j N_0)}{m_b(l_{n-1}, \beta^{n-1} N_0)}. \tag{5.9}$$ {ci}

In view of (2.5) and (2.6), χ_j is given by

$$\chi_j = \left(2\sqrt{\beta}\right)^j \chi_0. \tag{5.10}$$ {chin1}

Thus, by (2.8) and (5.10), $\Delta\mu_n$ can be written as

$$\Delta\mu_n = \left(\frac{\sqrt{\beta}}{2}\right)^{n-1} \Delta\tilde{\mu}(\chi_{n-1}, \beta, \tan\alpha) \tag{5.11}$$ {del}

where

$$\begin{aligned} \Delta\tilde{\mu}(\chi_{n-1}, \beta, \tan\alpha) &= \beta \max\left\{\tfrac{1}{2\sqrt{\beta}}, \chi_{n-1}\right\} - \max\{1, \chi_{n-1}\} \\ &+ \chi_{n-1}(\beta-1)(1+\tan^2\alpha) \\ &+ (\beta-1)\tan^2\alpha \max\left\{\tfrac{(\tan\alpha)^{\frac{1}{2}}}{2\sqrt{\beta-1}}, \chi_{n-1}\right\}. \end{aligned} \tag{5.12}$$ {delchild}

Here, in view of the optimality conditon (4.4), $\beta = \eta^{-1}(\tan\alpha)$, with $\tan\alpha > 0$.

Now, let us denote by $n^* - 1$ the first complexity degree for which the horizontal struts undergo material failure, so that, by definition (5.9), $\chi_{n^*-1} \geq 1$ and, by (5.11) and (5.12), $\Delta\mu_{n^*-1} > 0$. In view of (5.10), for any $n > n^*$ we have $\chi_{n-1} > \chi_{n^*-1} \geq 1$ and, again by (5.11) and (5.12), $\Delta\mu_n > 0$ (see Fig.10a). Then the optimal complexity n_{opt} verifies the inequality $n_{opt} \leq n^* - 1$.

As a consequence, $n^* - 1$ is determined as the minimum positive integer such that $n^* - 1 \geq \mathrm{int}(\nu)$, where ν, defined by (5.7), is the real positive number for which it is satisfied the condition

$$\chi_\nu = \chi_0 (2\sqrt{\beta})^\nu = 1. \tag{5.13}$$ {ii}

Thus we have $n^* = 1 + \mathrm{int}(\nu)$. □

Proposition 2 *There exist a value $\bar{\varepsilon}$ of the parameter ε and an open interval $I_\varepsilon = (\alpha_1(\varepsilon),\ \alpha_2(\varepsilon))$ of the angle α such that for $\alpha \in I_\varepsilon$ with $\varepsilon \leq \bar{\varepsilon}$, it results*

$$n_{opt} \geq \mathrm{int}\,(\nu). \tag{5.14}$$ {resres}

Proof. We begin by observing that $\Delta\tilde{\mu}$ is an increasing function of both χ and $\tan\alpha$. Morover, since the optimal prestrecth parameter $\beta = \eta^{-1}(\tan\alpha)$ decreases as ε decreases, we have that $\Delta\tilde{\mu}$ *decreases as ε decreases* (see the scheme in the Fig.10b).

Now, in order to prove the proposition, we evaluate $\Delta\tilde{\mu}$ at $\chi = \frac{1}{2\sqrt{\beta}}$, which corresponds, in view of (5.10), to the (*non integer*) complexity $j = \nu - 1$. First, we want to show that at this (non integer) complexity, for any $\varepsilon < \bar{\varepsilon}$, where $\bar{\varepsilon}$ is a suitable value of ε, we always find an interval I_ε such that if $\alpha \in I_\varepsilon$ then we have $\Delta\tilde{\mu} < 0$. To this end in Fig.10b we represent the dependence of $\Delta\tilde{\mu}$, evaluated at $\chi = \frac{1}{2\sqrt{\beta}}$, on α for three different values of ε (corresponding to $\varepsilon = 10^{-3}, 10^{-2}, 5 * 10^{-2}$). Fig.10b shows the existence of I_ε and, since $\Delta\tilde{\mu}$ decreases as ε decreases, that the amplitude of the interval I_ε grows as ε decreases.

Finally, we observe that, as consequence of the monotonicity of χ and of $\Delta\tilde{\mu}$, if $\alpha \in I_\varepsilon$ then $\Delta\tilde{\mu} < 0$ also at the integer complexity $\mathrm{int}(\nu) - 1$ (see Fig.10a). This, in view of (5.8) and (5.11), implies that $\mu_{int(\nu)} < \mu_{int(\nu)-1}$, so that the optimal complexity n_{opt} must satisfies the relation $n_{opt} \geq \mathrm{int}\,(\nu)$. □

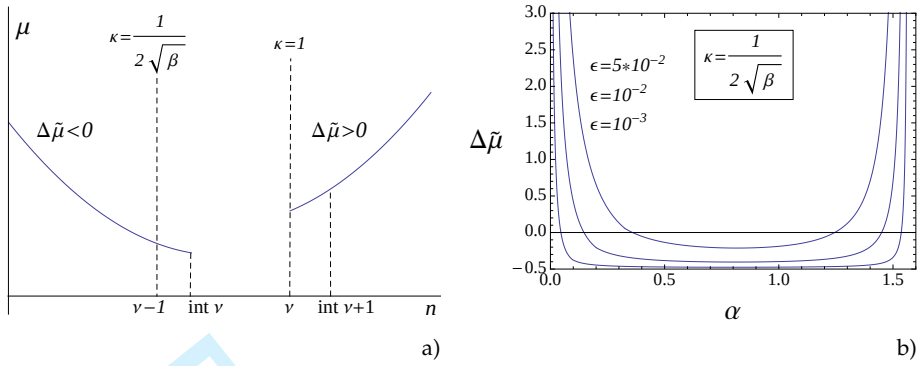

Figure 10. a) Scheme of the monotonicity properties of the mass μ with respect to the complexity order n. b) Evaluation of the domains I_ε where $\Delta\tilde{\mu}$ at $\chi = \frac{1}{2\sqrt{\beta}}$ is negative for different values of ε. In particular we find $I_{10^{-3}} = (0.0015\pi, 0.489\pi)$, $I_{10^{-2}} = (0.047\pi, 0.461\pi)$, $I_{5*10^{-2}} = (0.115\pi, 0.396\pi)$.

{fig10b}

Funding statement. The work G.P. and D.D. has been supported by Fondi di Ricerca di Ateneo of Politecnico di Bari.

References

1. Skelton, R.E., de Oliveira M.C.: Tensegrity systems, Springer (2009).
2. Donald, E., Ingber, N. W., Dimitrije S.: Review Article Tensegrity, cellular biophysics, and the mechanics of living systems, Journal of the Rep. Prog. Phys. 77, 046603 (2014).
3. Skelton, R.E., Fraternali, F., Carpentieri, G., Micheletti, A.: Minimum mass design of tensegrity bridges with parametric architecture and multiscale complexity, Mech. Res. Comm. 58, 124–132 (2014).
4. Paul, C., Valero-Cuevas, F.J.: Design and Control of Tensegrity Robots for Locomotion, IEEE Transaction on Robotics, 22, 944–957 (2006).
5. Sultan, C.,m, Skelton, R.: A force and torque tensegrity sensor, Sensors and Actuators A 112, 220–231 (2004).
6. Djouadi, S., Motro, R., Pons, J., Crosnier, B.: Active Control of Tensegrity Systems, J. Aerosp. Eng., 11(2), 37–44 (1998).
7. Bazaraa, M.S., Sherali, H. D., Shretty, C. M., 2006. Nonlinear programming. Theory and Algorithms Third Edition. J. Wiley.
8. Caluwaerts Ken and Carbajal Juan Pablo, "Energy conserving constant shape optimization of tensegrity structures. International Journal of Solids and Structures", 2015, ISSN 0020-7683, doi:10.1016/j.ijsolstr.2014.12.023
9. C. Sultan and R. Skelton: Deployment of tensegrity structures. International Journal of Solids and Structures, 40 (2003), 4637–4657.
10. A.G. Tibert and S. Pellegrino: Deployable tensegrity reflectors for small satellites. Journal of Spacecraft and Rockets (AIAA), 39 (2002), 701–709.
11. K.Yu. Volokh, O. Vilnay, and M. Belsky: Tensegrity architecture explains linear stiffening and predicts softening of living cells. Journal of Biomechanics, 33 (2000), 1543–1549.
12. R. Motro: Tensegrity (Kogan Page Science, London, 2003).
13. R.B. Fuller: Synergetic: Explorations in the Geometry of Thinking, Collier McMillian,London, 1975
14. Skelton, R.E., Fraternali, F., Carpentieri, G., Micheletti, A.: Minimum mass design of tensegrity bridges with parametric architecture and multiscale complexity, Mech. Res. Comm. 58, 124–132 (2014).
15. Puglisi G., Truskinovsky L. Mechanics of a discrete chain with bi-stable elements, Journal of the Mechanics and Physics of Solids, 48, Issue 1, 2000, Pages 1-27
16. K. A. Lazopoulos. Stability of an elastic tensegrity structure, Acta Mechanica, 179, Issue 1-2, January 2005, Pages 1-10

17. F. Trentadue. Minimum weight design of non-linear elastic structures with multimodal buckling constraints, International Journal for Numerical Methods in Engineering Volume 56, Issue 3, pages 433–446, 21 January 2003
18. K. Nagase, R. E. Skelton. Minimal mass design of tensegrity structures. Proc. SPIE 9061, Sensors and Smart Structures Technologies for Civil, Mechanical, and Aerospace Systems 2014, 90610W; doi:10.1117/12.2044869
19. D. De Tommasi, G. Puglisi, G. Zurlo. Inhomogeneous spherical configurations of inflated membranes. Continuum Mech. Thermodyn. (2013) 25:197–206 DOI 10.1007/s00161-012-0240-2
20. D. Sornette. Critical Phenomena in Natural Sciences Chaos, Fractals, Selforganization and Disorder: Concepts and Tools (2003) Springer. ISBN 978-3-540-33182-7
21. D. Markovic, C. Gros.Power laws and self-organized criticality in theory and nature. Physics Reports. (2014) 536: 41–74
22. L. Puig, A. Barton, N. Rando. A review on large deployable structures for astrophysics missions. Acta Astronautica 67(2010)12–26
23. D. Rayneau-Kirkhope, Y. Mao, and R. Farr. Ultralight Fractal Structures from Hollow Tubes. Phys. Rev. Lett. 109 (2012), 204301.

rspa.royalsocietypublishing.org Proc R Soc A 0000000